# PolSAR Image Filtering based on Feature Detection using the Wavelet Transform

Grégory Farage[1, 2]
CARTEL[1]
University of Sherbrooke
Sherbrooke, QC, Canada
gregory.farage@usherbrooke.ca

Samuel Foucher[2], Goze B. Bénié[1]
Computer Research Institute of Montreal[2]
Montreal, QC, Canada
sfoucher@crim.ca
gbenie@usherbooke.ca

*Abstract*— **This paper elucidate a new approach for speckle reduction in polarimetric synthetic aperture radar ("PolSAR") images based on the stationary wavelet transform. Noisy wavelet coefficients are thresholded using an entropic thresholding technique. Principal Component Analysis and Sum of Squared Coefficients methods are used to detect significant coefficients based on the entire polarimetric covariance matrix.**

***PolSAR, speckle filtering, wavelet, entropic thresholding.***

## I. INTRODUCTION

In the last decade, many theoretical developments in multiresolution analysis have been considered. Wavelets showed successful results in many applications to alleviate a variety of signal processing problems, such as image compression and image denoising. In PolSAR filtering window based algorithm, the trade-off between noise reduction and spatial features preservation is highly dependent on the size of the window. There exist few filters that are able to adapt the size or the shape of the filtering window according to the underlying structural features, such as the refined Lee filter [1]. However, wavelet multiresolution analysis presents a very useful property of space and scale localization, as it identifies homogeneous areas and localized structures according to scales. For polarimetric SAR images, De Grandi [2] used a wavelet multi-resolution representation to provide a unified framework for signal approximation, filtering and classification. He demonstrated that wavelet method reaches finer results in preserving points targets and small linear features. More recently De Grandi [3] presented a technique for texture analysis and segmentation of PolSAR data based on a wavelet decomposition.

In this paper, a multiscale PolSAR image filtering technique is proposed by identifying significant wavelet coefficients (i.e. mainly those generated by edges and point targets). We apply the wavelet transform to each element of the covariance matrix, and use its full polarimetric information to classify the wavelet coefficients (i.e. not only the power bands). Two different approaches in the wavelet domain are explored to achieve an improved detection: the Principal Component Analysis ("PCA") and a combinatory signal inter-band, derived from [4]. The main purpose of PCA is to find a suitable representation of multivariate data in order to make the essential structure more visible and to identify any distinct feature. Alternatively, the concept surrounding the inter-band combination is that in lieu of processing each band individually, the high correlation potentially existing between multivalued bands is exploited. Once the coefficients are enhanced, we detect the feature of the PolSAR data by applying an entropic thresholding.

This paper is organized as follows. In section II, a background information relating to feature detection and thresholding is provided. In section III, simulations are carried out to investigate the performances of the presented approach. Filtered artificial and real images are also showed.

## II. WAVELET FEATURES DETECTION OF POLSAR IMAGES

In reciprocal backscattering case, $S_{hv} = S_{vh}$, polarimetric information can be represented by the scattering vector $\boldsymbol{k_S}$,

$$\mathbf{k}_S = \begin{bmatrix} S_{hh} & \sqrt{2}S_{hv} & S_{vv} \end{bmatrix}^T \tag{1}$$

where $h$ and $v$ represent respectively the transmitting horizontal and receiving vertical linear polarization, and the superscript "$T$" refers to the matrix transpose. From (1), the polarimetric covariance matrix $\mathbf{C}$ and the span are expressed as follows,

$$\mathbf{C} = \mathbf{k}_S \mathbf{k}_S^{*T} \tag{2}$$

$$span = \mathbf{k}^{*T}\mathbf{k} = |S_{hh}|^2 + 2|S_{hv}|^2 + |S_{vv}|^2 \tag{3}$$

where the superscript "*" refers to the complex conjugate. A more convenient form of the covariance matrix $\mathbf{C}$, used in the next sections, is defined such that:

$$\begin{aligned} \mathbf{I} = \big[ & \mathbf{C}_{11}, \mathbf{C}_{22}, \mathbf{C}_{33}, \\ & \Re e\{\mathbf{C}_{12}\}, \Re e\{\mathbf{C}_{13}\}, \Re e\{\mathbf{C}_{23}\}, \\ & \Im m\{\mathbf{C}_{12}\}, \Im m\{\mathbf{C}_{13}\}, \Im m\{\mathbf{C}_{23}\} \big] \end{aligned} \tag{4}$$

### A. *Wavelet besed Structure Detection*

The main objective is to detect features related to edges and point targets, and then to filter PolSAR data by taking advantage of the features detection. The wavelet transform employed in the following equations is based on a *Stationary Wavelet Transform* (SWT) used by Foucher [5] for the multiscale filtering of SAR images. The wavelet transform of each band $I_n$ of the PolSAR data is composed of $3J$ high-frequency images defined as $\{W_\varepsilon^{[j]} I_n\}_{\varepsilon=h,v,d}^{j=1,\ldots,J}$ and $J$ low-frequency images $\{A^{[j]} I_n\}^{j=1,\ldots,J}$. The wavelet transform of an image $I_n$ is then defined by

$$W^{[j]} I_n = I_n * \psi^{[j]} \tag{5}$$

where $\psi^{[j]}$ is the wavelet at level $j$, and we denote "*" as the convolution operator. In order to enhance the significant coefficients in the high-frequency images and to offer some robustness to speckle noise we use the following operator:

$$M^{[j]} I_n = \frac{\sqrt{L}}{A^{[j]} I_n} \sqrt{\sum_{\varepsilon=h,v,d} \frac{\left(W_\varepsilon^{[j]} I_n\right)}{S_{2,\varepsilon}^{[j]}}} \tag{6}$$

where $S_{2,\varepsilon}^{[j]}$ is the wavelet power gain [5]. The interest of this operator is illustrated in Figure 1, which has been designed so that the span does not contain any significant (weak or nonexistent) feature information, Figure1 (b). However, the operator (6) is able to detect some features on the power band, Figure1 (c), and on the complex bands Figure1 (d).

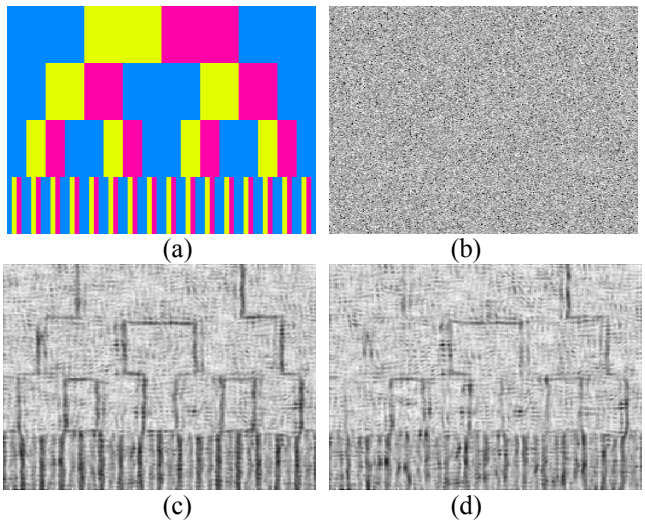


Figure 1. Simulated PolSAR: images (a) Ground Truth image R =|Shv|² G=|Svv|² B=|Shh|²; (b) One look span image; (c) $\sum_{n=1}^{3} M^{[3]} I_n$; (d) $\sum_{n=4}^{9} M^{[3]} I_n$.

Moreover, we regard $M^{[j]} I_n$ as the root square of a sum of three independent centered random variables, which implies that the probability density function (pdf) should be close to a scaled $\chi$ distribution with 3 degrees of freedom [5]. In the following sections, an attempt to maximize and threshold the significant coefficients will be conducted.

### B. *Enhancement of the Significant Wavelet Coefficients*

In order to enhance the significant coefficients values, we use principally two different techniques: the Principal Component Analysis (PCA) and the Sum of Squared Coefficients (SSC).

The PCA is one statistical method often used with hyperspectral images to capture the significant information contained in high dimensionality [6]. In an analogous way, we use PCA on wavelet coefficients to maximize edge energy in the reduced polarimetric dimension images. Then we apply the principal component and a hard thresholding method detailed in the next section to produce a binary mask that will select the significant wavelet coefficients at a particular resolution and exclude the noise related wavelet coefficients.

An alternative technique to boost the significant wavelet coefficients is to employ a denoising strategy of multivalued images, presented by Scheunders [4], and apply a wavelet thresholding method where the correlation between different wavelet scales and bands are exploited. In our approach, a threshold value is derived using a wavelet entropy thresholding technique.

Schaunders proposed to make use of the high correlation that generally exists among the multivalued bands, rather than of treating each band separately. We take advantage of the signal interband correlation to differentiate noise from signal. In order to accomplish this, we use the *Sum of Squared Coefficients* (SSC). By squaring real edge coefficients tend to become larger for coarser scales, while noise coefficients become smaller. Following, the thresholding procedure for all bands is given as the following,

$$\begin{cases} g^{[j]} = 1, \text{ if } \sum_{n=1}^{N} \left(M^{[j]} I_n\right)^2 > \bar{T} \\ g^{[j]} = 0, \quad \text{otherwise} \end{cases} \tag{7}$$

where $g^{[j]}$ is the significant wavelet coefficient mask, and $\bar{T}$ is the threshold value defined via a non parametric technique, described below.

### C. *Entropy based Wavelet Thresholding*

The entropy is an uncertainty measure first introduced by Shannon in his information theory to describe how much information is enclosed in a source ruled by a probability law. This concept becomes increasingly important in image processing due to the fact that an image can be interpreted as an information source with the probability law given by its image histogram.

The entropic thresholding technique provides an automatic way to obtain an optimal threshold depending on the image contents. Fan *et al.* [7] showed the efficiency of this technique for a two class data classification: edge and non-edge problem. Given an input high-frequency wavelet image, let us assume

that the values of the pixels have a range [*0, M*] and $f_i$ is the number of pixels having the value *i*, $i \in [0, M]$. The pixel value of the high-frequency image can be considered as an edge strength feature value. For a given threshold, *e.g. T*, $P_n(i)$ and $P_e(i)$ describe respectively the probability for non-edge and edge pixels, whose distributions are independent.

$$P_n(i) = \frac{f_i}{P_0(T)},\ 0 \le i \le T \tag{8}$$

$$P_e(i) = \frac{f_i}{P_1(T)},\ T+1 \le i \le M \tag{9}$$

Where $P_0(T)$ represents the total number of pixels that have values in range of [*0, T*] and $P_1(T)$ is the total number of pixels whose values are in range of [*T+1, M*]. Thus the entropies are given as follows

$$H_n(T) = -\sum_{i=0}^{T} P_n(i) \log P_n(i) \tag{10}$$

$$H_e(T) = -\sum_{i=T+1}^{M} P_e(i) \log P_e(i) \tag{11}$$

Then, in order to obtain the desirable threshold for an edge-non-edge classification, Cheng *et al.* [8] suggested satisfying the following criterion function

$$H(\tilde{T}) = \max_{T=0,1,2,...M} \{H_n(T) + H_e(T)\} \tag{12}$$

Based on the recursive iteration property of both entropies, Fan *et al.* [7] proposed the following computation to get an optimal threshold,

$$\begin{aligned} H_n(T+1) = &\frac{P_0(T)}{P_0(T+1)} H_n(T) - \frac{f_{T+1}}{P_0(T+1)} \log \frac{f_{T+1}}{P_0(T+1)} \\ &- \frac{P_0(T)}{P_0(T+1)} \log \frac{P_0(T)}{P_0(T+1)} \end{aligned} \tag{13}$$

$$\begin{aligned} H_e(T+1) = &\frac{P_1(T)}{P_1(T+1)} H_e(T) - \frac{f_{T+1}}{P_1(T+1)} \log \frac{f_{T+1}}{P_1(T+1)} \\ &- \frac{P_1(T)}{P_1(T+1)} \log \frac{P_1(T)}{P_1(T+1)} \end{aligned} \tag{14}$$

Since points targets produce very large wavelet coefficients that must be preserved [5][9], a target threshold is imposed such that

$$\begin{cases} g^{[j]} = 1, \text{ if } ECM\left\{M^{[j]} I_n\right\}^{n=1,2,3} > \sqrt{L+2} \\ g^{[j]} = 0, \qquad \text{otherwise} \end{cases} \tag{15}$$

where, $g^{[j]}$ is the binary mask for the level *j*, ECM is defined as an Enhancement Coefficient Method (PCA or SSC) and *L* is the PolSAR image number of looks. Moreover, in order to extend the homogenous areas through the scales, masks are combined iteratively,

$$g^{[j]} = g^{[j]} \times g^{[j+1]},\ \text{with } j = J-1,...,1 \tag{16}$$

In Figure 2, examples of masks through 3 levels are shown as well as the extension of the homogeneous areas. Once the masks are obtained, the wavelet coefficients are multiplied by the shrinkage function.

$$\left(W^{[j]} I_n\right)' = g^{[j]} \times W^{[j]} I_n \tag{17}$$

Magnitude of the wavelet coefficients corresponding to significant image features or edges is known to increase with a larger scale. On the other hand, magnitudes of wavelet coefficients contributing mainly to noise decrease with the level.

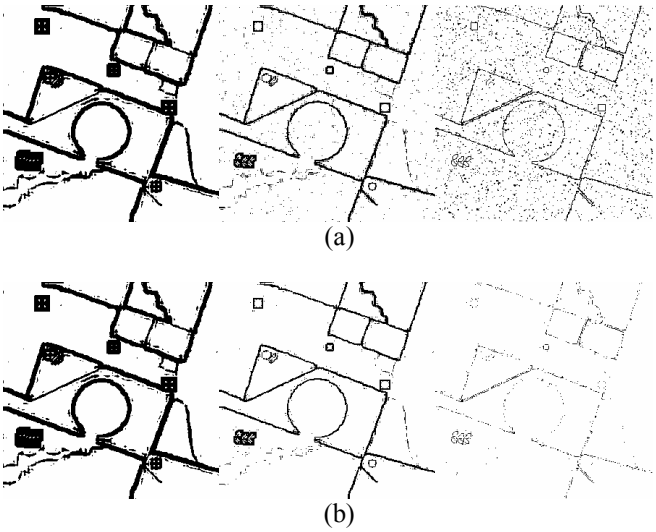


Figure 2. Masks computed with SSC from level 3, left, to level 1, right (a) Mask without extension (b) Mask with extension. White means zero value.

### *D. Despeckling Method*

The various steps of the full non-parametric filtering method are enumerated below:

1. Carry out the stationary wavelet transform of the PolSAR covariance matrix in *J* levels, obtaining 3*J* high-frequency images and *J* low-frequency images.
2. Enhance significant wavelet coefficients by applying PCA or SSC on the span, on the sum of off-diagonal, or on all elements.
3. Classify the edge and non-edge coefficients, using entropy thresholding and the shrinkage function.
4. Modify the wavelet coefficients by multiplying by the mask function $g^{[j]}$.
5. Apply the inverse wavelet transform on the modified wavelet coefficients, producing the filtered image.

## III. RESULTS

### A. Experiments Using Simulated Images

The performances of analyses are evaluated on simulated PolSAR images, produced from the Cholesky factorization of samples of typical polarimetric responses.

Speckle reduction performances are evaluated on simulated PolSAR images (single look complex), produced from the Cholesky factorization [10] of typical samples polarimetric responses. Five areas with different scattering properties are selected within an E-SAR image (L-band, DLR, Oberpfaffenhofen area).. The final PolSAR image is shown on Figure 3, in addition to the ground truth image. For the proposed method, wavelet coefficients are quantized on $M=256$ levels for the computation of the entropy threshold and a Biorthogonal-5 wavelet basis is used. We evaluate the performances of the artificial PolSAR image filtering on its three power bands with the following indicator:

- *Equivalent number of looks* (ENL): a measure that indicates the strength of the noise reduction; we compute the ENL for each power channel and each scattering classes (we exclude point targets) and we take the mean value.

$$ENL = \frac{1}{3\times 5}\sum_{n=1,2,3}\sum_{l=1,..,4}\frac{E\left[(I_n - < I_n >)^2 \mid l\right]}{< I_n >^2} \qquad (18)$$

- *Edge strength preservation* (EP): preservation of the edge magnitudes of filtered image is compared to the ground truth image (the smaller the EP the more significant it is).

$$EP = \frac{1}{3\times 5}\sum_{n=1,...,3}\sum_{l=1,...,5}\left|1-\frac{\sum_{\mathbf{x}\in Edges}\left\|\nabla I_n(\mathbf{x})\right\|}{\sum_{\mathbf{x}\in Edges}\left\|\nabla I_n^{GT}(\mathbf{x})\right\|}\right| \qquad (19)$$

Table 1 shows the results obtained for both three and four levels of decomposition for the stationary wavelet transform with Biorthogonal-5 wavelet basis. The enhanced Lee filter was applied with a 9x9 window.

TABLE I. FILTERING PERFORMANCES.

| Filter | 3 Levels | | 4 Levels | |
|---|---|---|---|---|
| | ENL | EP | ENL | EP |
| Sum power bands | 24.87 | 0.3042 | 34.65 | 0.3361 |
| Sum of complex bands | 23.73 | 0.3086 | 32.57 | 0.3395 |
| PCA based on power bands | 26.73 | 0.3300 | 10.77 | 0.6392 |
| PCA based on complex bands | 25.59 | 0.3439 | 12.77 | 0.6139 |
| PCA based on all bands | 25.90 | 0.3312 | 11.91 | 0.1422 |
| SSC based on power bands | 14.60 | 0.1312 | 16.42 | 0.1422 |
| SSC based on complex bands | 12.32 | 0.1050 | 13.90 | 0.1139 |
| SSC based on all bands | 16.27 | 0.1347 | 20.27 | 0.1514 |
| Enhanced Lee | 14.47 | 0.3826 | 14.47 | 0.3826 |

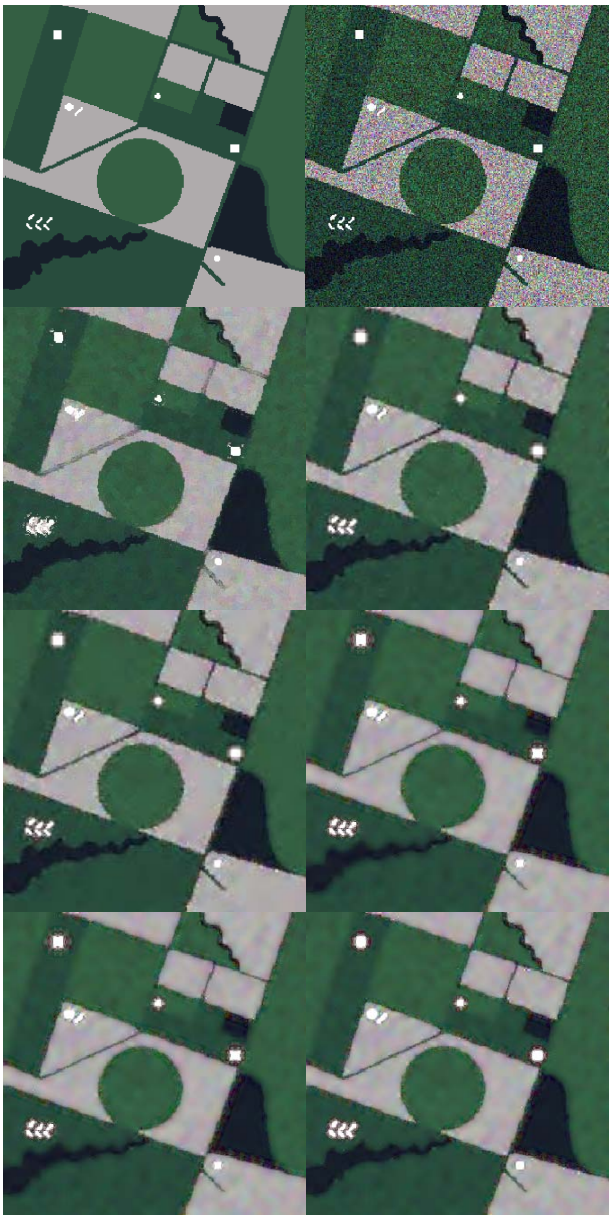

Figure 3. Display color, red = $\sqrt{2}$ |Shv|$^2$ , green = |Svv|$^2$, blue = |Shh|$^2$, and from left to right and top to bottom : ground truth, original image, enhanced Lee (9x9), SSC on all bands with 4 levels, SSC on all bands with 3 levels, PCA on all bands with 3 levels, PCA on all bands with 4 levels, power bands with 4 levels.

### B. *ExperimentsUsing PolSAR Images from Airborne Sensor*

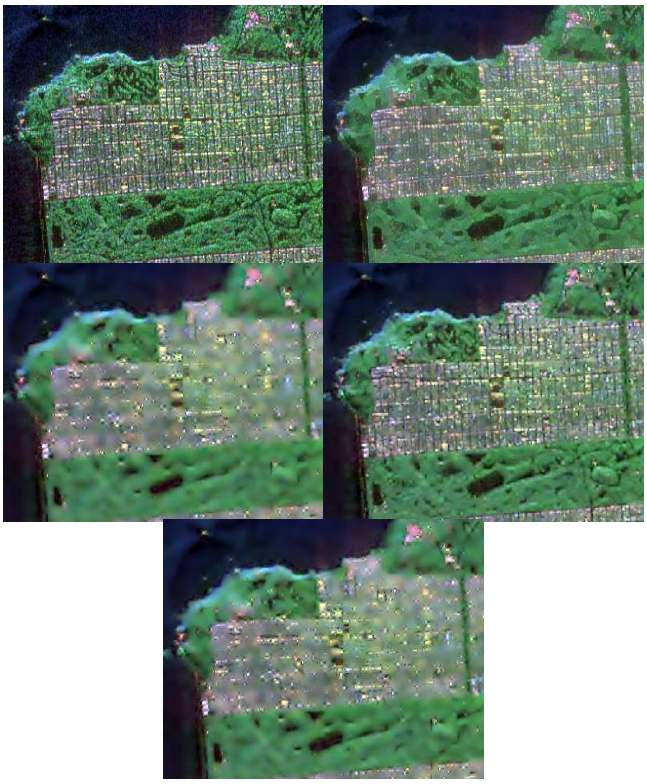

Figure 4. Display is obtained by a Pauli decomposition, and from left to right and top to bottom : original image, enhanced Lee (9x9), PCA on all bands with 3 levels, SSC on all bands with 4 levels, power bands with 3 levels.

In case of real images, the filters were applied to the National Aeronautics and Space Administration Jet Propulsion Laboratory (NASA/JPL) AIRSAR L-band POLSAR data of a San Francisco image. These data were originally four-look processed by averaging the Stokes matrices.

## IV. Discussion and Conclusion

It can be seen from Table 1 that PCA offers higher ENL values compared to the others filters, and PCA EP values remain lower than EP value of the enhanced Lee filter. However, the SSC method provides better results overall regarding the edge preservation. As the number of levels increases, the Table 1 clearly demonstrates that SSC results are improved, but the performances of PCA are immensely degraded. Alternatively, it is interesting to note that by combining the complex bands, the performances of the power bands based SSC improved. Reviewing the simulated images, one can observe that all filters have distorted or enlarged targets. Particularly, PCA based filtering indicates some significant artifacts around the strong targets, which is a common phenomenon while applying wavelet decomposition to strong targets. Not only does the SSC provide satisfying speckle reduction but it also presents a remarkable capacity to retain edges and meaningful spatial features. When applied to real images Figure 4, the SSC demonstrates a respectable tendancy to smooth homogeneous areas while preserving spatial features. However, the PCA oversmooths the homogenous regions, and consequently alters any spatial features. Its non-parametric property combined with the SSC algorithm yields encouraging results for the entropic thresholding technique. As such it will be the subject of future studies.

## Acknowledgment

This work has been supported in part by the NSERC of Canada (Discovery Grant) and the MDEIE of the "Gouvernement du Québec". The authors wish to thank the DLR (German Aerospace Center) for so graciously providing them with the E-SAR dataset.

## References

[1] J.S. Lee, M. R. Grunes, and G. De Grandi, "Polarimetric SAR Speckle Filtering and its Implication for Classification", *IEEE Trans. Geosci. Remote Sensing*, Vol. 37, No 5, pp 2363-2373, Sep. 1999.

[2] G. De Grandi, J.-S. Lee, M. Simard, H. Wakabayashi, D. Schuler, and T. Ainsworth, "Speckle filtering, segmentation and classification of polarimetric SAR data: a unified approach based on the wavelet transform", *Proc. IGARSS*, Vol. 3, , pp 1107-1109, July. 2000.

[3] G. De Grandi, D. Hoekman, J.-S. Lee, D. Schuler, and T. Ainsworth, "A Wavelet multiresolution technique for polarimetric texture analysis and segmentation of SAR images", *Proc. IGARSS*, Vol. 1, Sept. 2004.

[4] P. Scheunders, "Wavelet thresholding of multivalued Images", IEEE *Trans. Image Processing*, Vol. 13, No 4, pp 475-483, April. 2004.

[5] S. Foucher, "Multiscale Filtering of SAR Images Using Scale and Space Consistency", *IGARSS*, Barcelona, Spain, 2007, to appear

[6] M.R. Gupta, and N.P. Jacobson, "Wavelet Principal Component Analysis and its Application to Hyperspectral Image", IEEE *ICIP*, Atlanta, October, 2006.

[7] J. Fan, R. Wang, L. Zhang, D. Xing, and F. Gan, "Automatic Image Segmentation by Integrating Color-Edge Extraction and Seeded Region Growing", *IEEE Trans. Image Processing*, Vol. 10, No. 10, pp 1454-1466, October, 2001..

[8] H.D. Cheng, Y.H. Chen, and X.H. Jiang, "Thresholding using two-dimensional histogram and fuzzy entropy principle", *IEEE Trans. Image Processing*, Vol. 9, pp. 732-735, 2000.

[9] S. Foucher, G. Farage, and G. B. Bénié, "SAR Image Filtering Based on the Stationary Contourlet Transform", IGARSS, Denver, pp. 4021-4024, Jul. 2006

[10] L. Pipia and X. Fàbregas, "Generation of Pol-SAR and Pol-In-SAR Data for Homogeneous Distributed Targets Simulation", In *Workshop on Polarimetric Synthetic Aperture Radar* (ESA SP-529), Frascati, Italy, 2005.